Supporting Information

Absolute handedness control of oligoamide double helices by chiral oxazolylaniline induction

Ling Yang,[a] Chunmiao Ma,[a] Brice Kauffmann,[b] Dongyao Li[a] and Quan Gan*[a]

[a]Hubei Key Laboratory of Bioinorganic Chemistry & Materia Medica, School of Chemistry and Chemical Engineering, Huazhong University of Science and Technology, Wuhan, 430074, P. R. China
[b]Université de Bordeaux, CNRS, INSERM, IECB–UMS3033–US001, Institut Européen de Chimie et Biologie, 2 rue Robert Escarpit, 33600 Pessac, France

Correspondence and requests for materials should be addressed to Quan Gan (ganquan@hust.edu.cn).

Table of Contents

1. X-ray Crystallography

Single crystal *S*-**2** was grown by slow diffusion of hexane into a chloroform concentrated solution. A single crystal of *S*-**2** in mother liquor was pipetted onto a glass containing Paratone-N oil. To avoid collapse of the crystal lattice, the crystal was quickly mounted onto a nylon loop and immediately flash cooled in liquid nitrogen.

Crystallographic data were all collected at Wuhan University on a Bruker Kappa Apex DUO diffractometer. Data were diffracted at the MoKα wavelength, and data-collection strategies were based on Phi and Omega scans at 100(2) K.

The structures were solved by direct methods using SHELXT[S1] and refined against F[S2] on all data by full-matrix least squares with SHELXL[2] following established refinement strategies.[S3] Most of the non-H atoms were refined with anisotropic temperature parameters, the disordered ones were refined with isotropic temperature parameters. All hydrogen atoms, were included into the model at geometrically calculated positions and refined using a riding model. SHELX ISOR, DELU, RIGU and SIMU restraints were used in the refinement strategy in order to reduce the anisotropic displacement parameters of the side chains. DFIX instructions were used to geometrically restraint most of the side chains. The contribution of the electron density associated with disordered solvent molecules, which could not be modelled with discrete atomic positions were handled using the SQUEEZE[S4] routine in PLATON. Crystallographic data have been deposited with the CCDC, under deposition number CCDC 2009252.

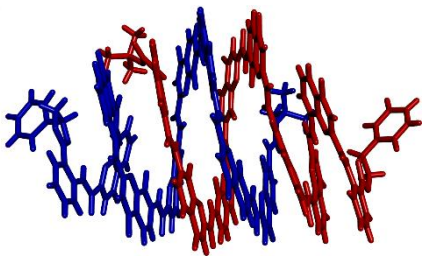

Fig. S1 The crystal structure of the chiral compound *S*-**2**. Solvent molecules and isobutoxy residues are omitted for clarity.

Table S1. Crystal data and structure refinement for the compound *S*-**2**.

Formula	C134 H130 Cl6 F6 N18 O19
M	2623.25
Crystal system	orthorhombic
Space group	$C222_1$
a/Å	35.445(7)
b/Å	36.434(7)
c/Å	45.806(9)
α/°	90
β/°	90
γ/°	90
V/Å^3	59154(21)
T /K	100
Z	16
ρ/g cm^{-1}	1.178
size (mm)	0.2 × 0.1 × 0.1
λ/ Å	0.720
μ/mm^{-1}	0.190
Independent reflections	53467
measured reflections	54007
parameters/restraints	3334/325
*R*1, *wR*2	0.1057, 0.3176
goodness of fit	1.291

2. Solution studies of chiral oligoamide foldamers

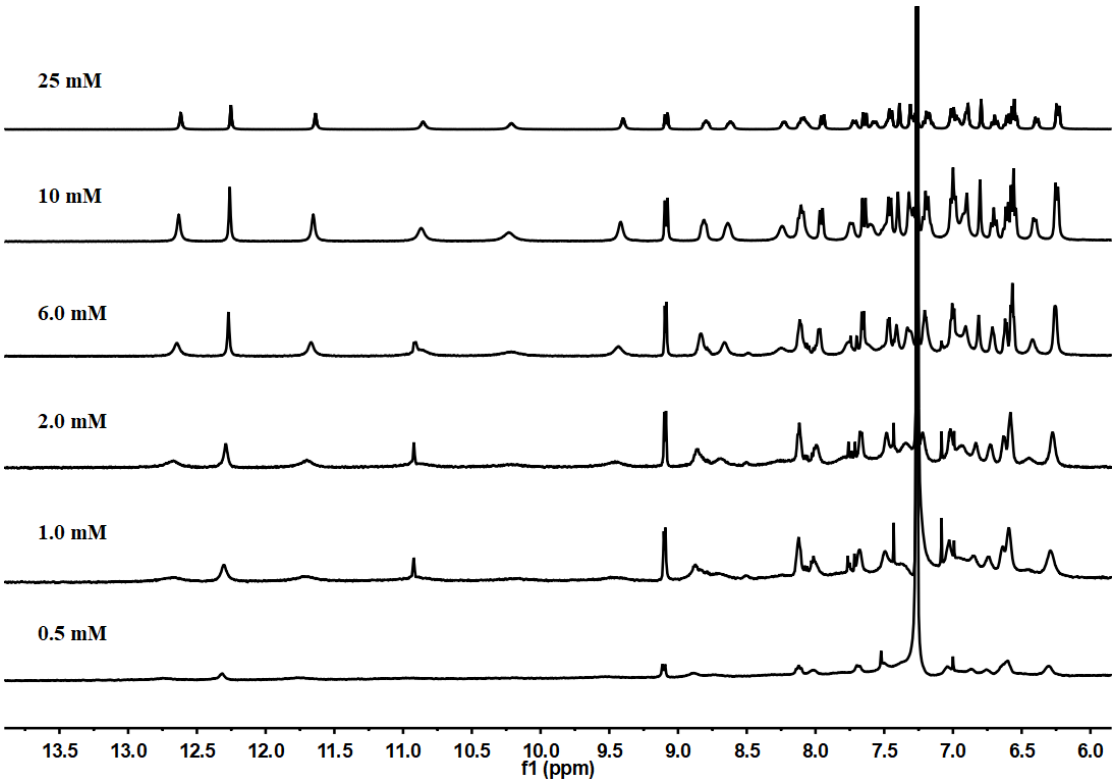

Fig. S2 Partial ^{1}H NMR (400MHz, 298 K) spectra of *S*-**1** upon changing the concentration in $CDCl_3$.

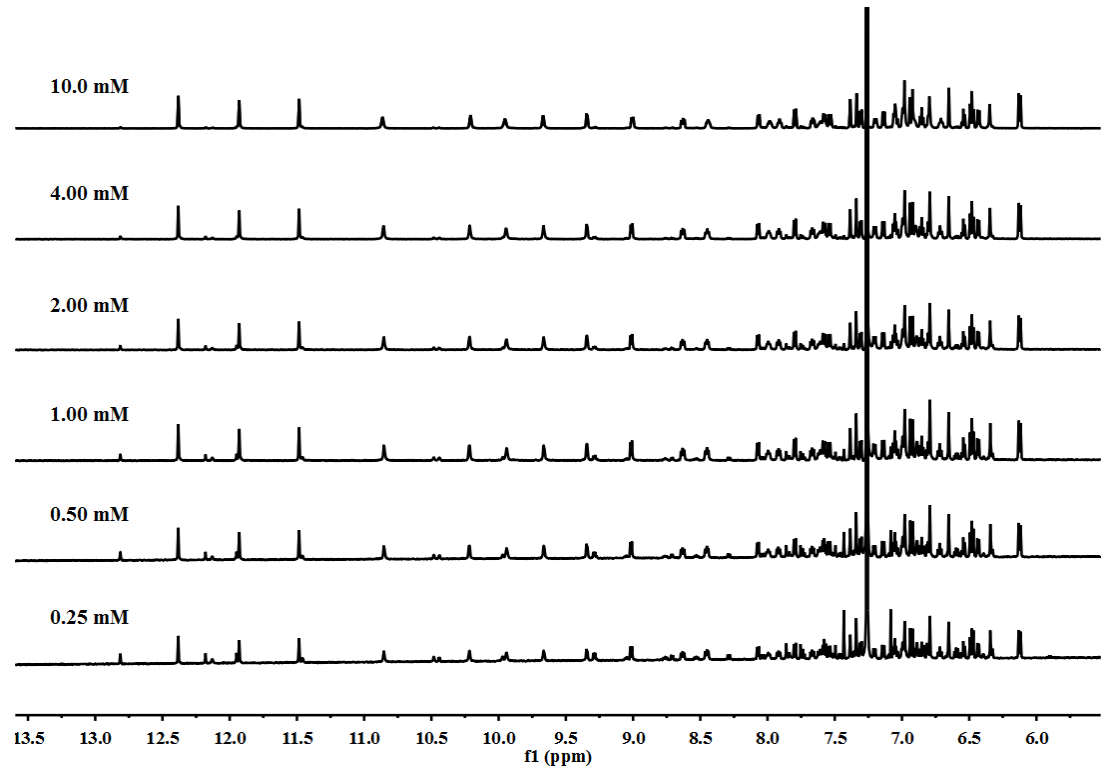

Fig. S3 Partial ^{1}H NMR (600MHz, 298 K) spectra of *S*-**2** upon changing the concentration in $CDCl_3$.

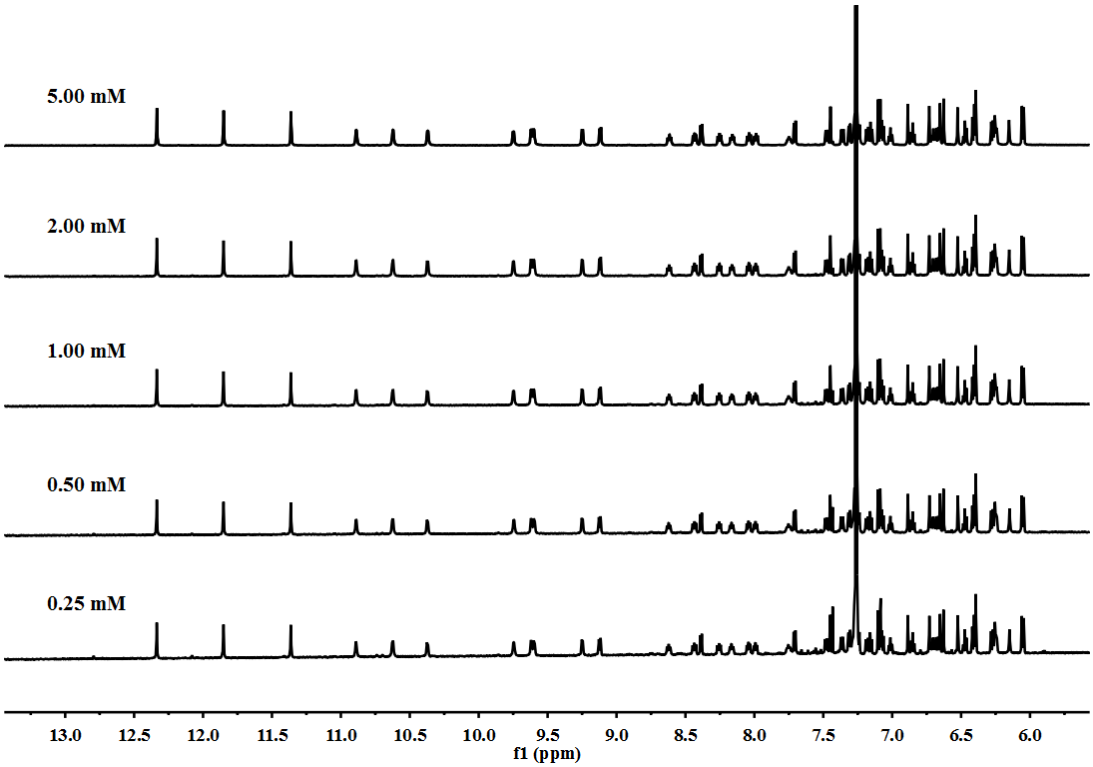

Fig. S4 Partial ^{1}H NMR (600MHz, 298 K) spectra of *S*-**3** upon changing the concentration in $CDCl_3$.

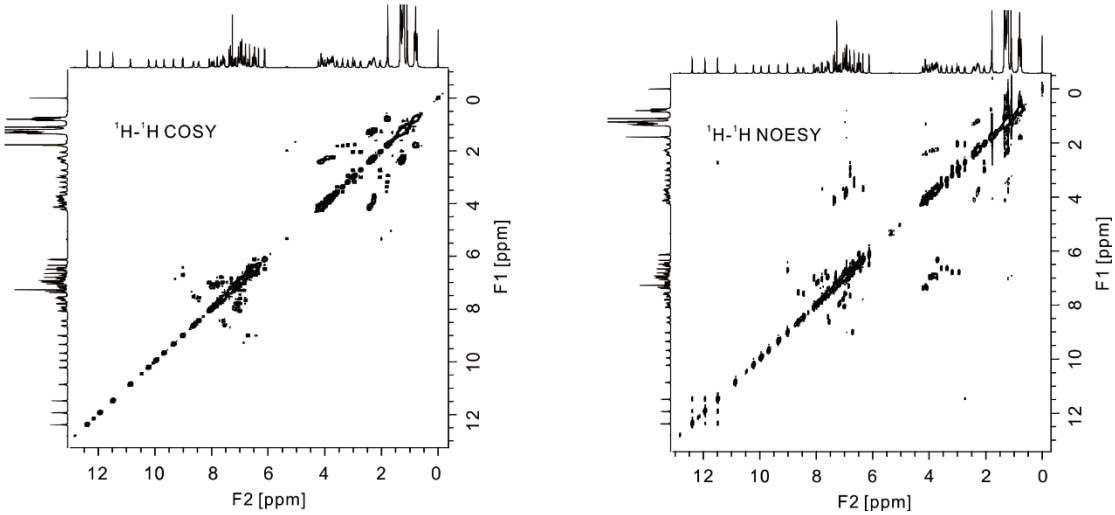

Fig. S5 The ^{1}H-^{1}H COSY and NOESY spectra of *S*-**2** in $CDCl_3$ (400MHz, 298 K, 20 mM).

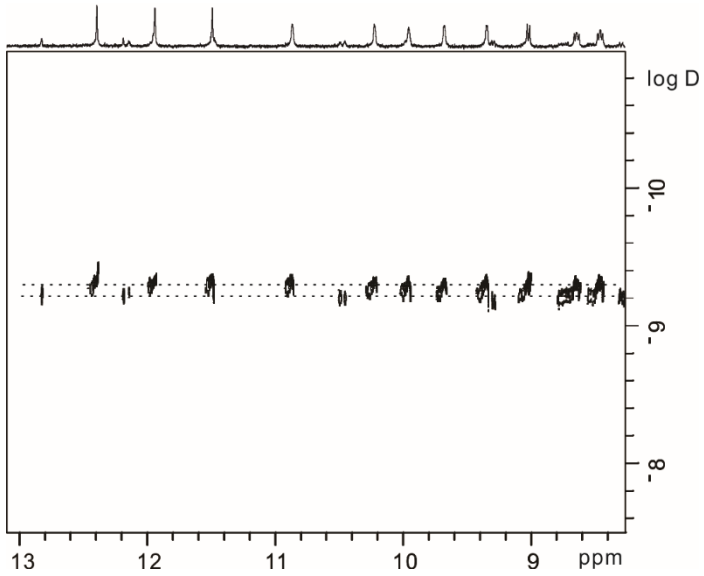

Fig. S6 The ^{1}H-^{1}H DOSY spectra of *S*-**2** in $CDCl_3$ (400MHz, 298 K, 1.0 mM).

3. Chiral optical characters of foldamers

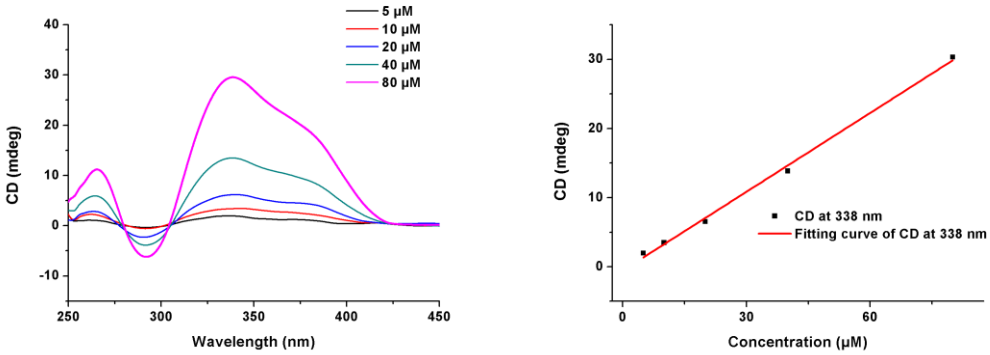

Fig. S7 a). Concentration-variation CD spectra of the compound *S*-**1**; b). the linear fit of CD data at 338 nm, the correlation factor is 0.996.

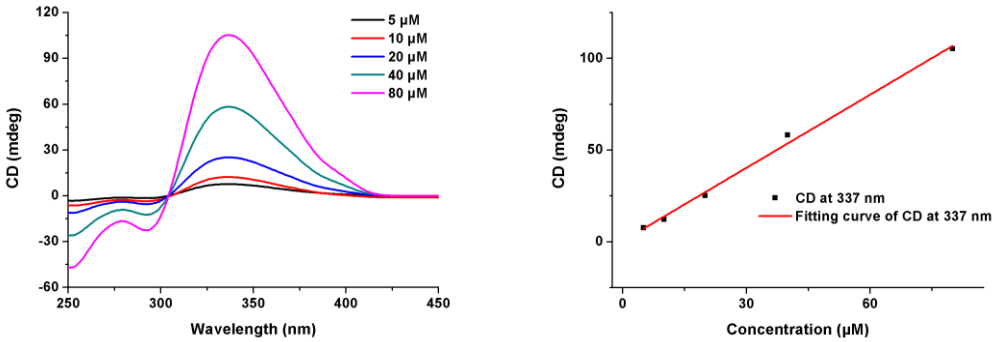

Fig. S8 a). Concentration-variation CD spectra of the compound *S*-**3**; b). the linear fit of CD at 337 nm, the correlation factor is 0.994.

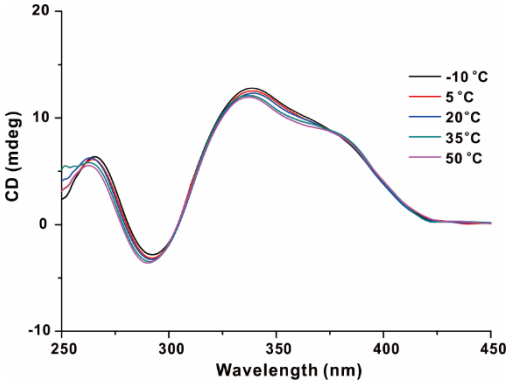

Fig. S9 Temperature-variation CD spectra of the compound *S*-**1** (40 μM).

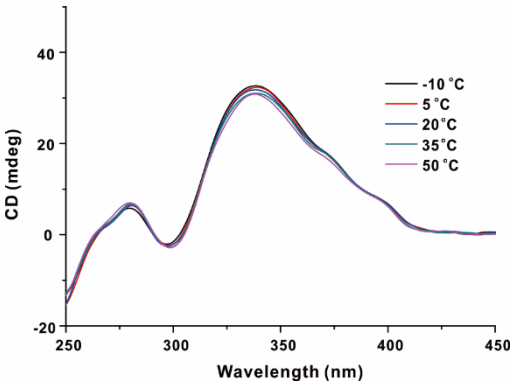

Fig. S10 Temperature-variation CD spectra of the compound *S*-**2** (40 μM).

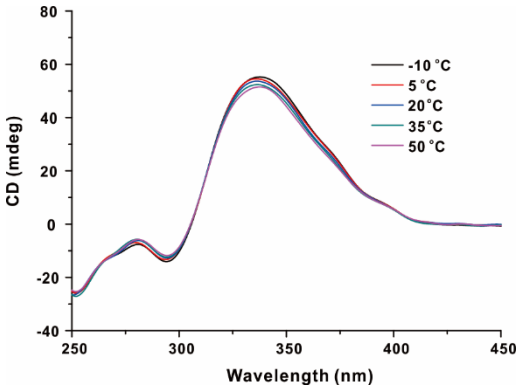

Fig. S11 Temperature-variation CD spectra of the compound *S*-**3** (40 μM).

4. NMR spectra

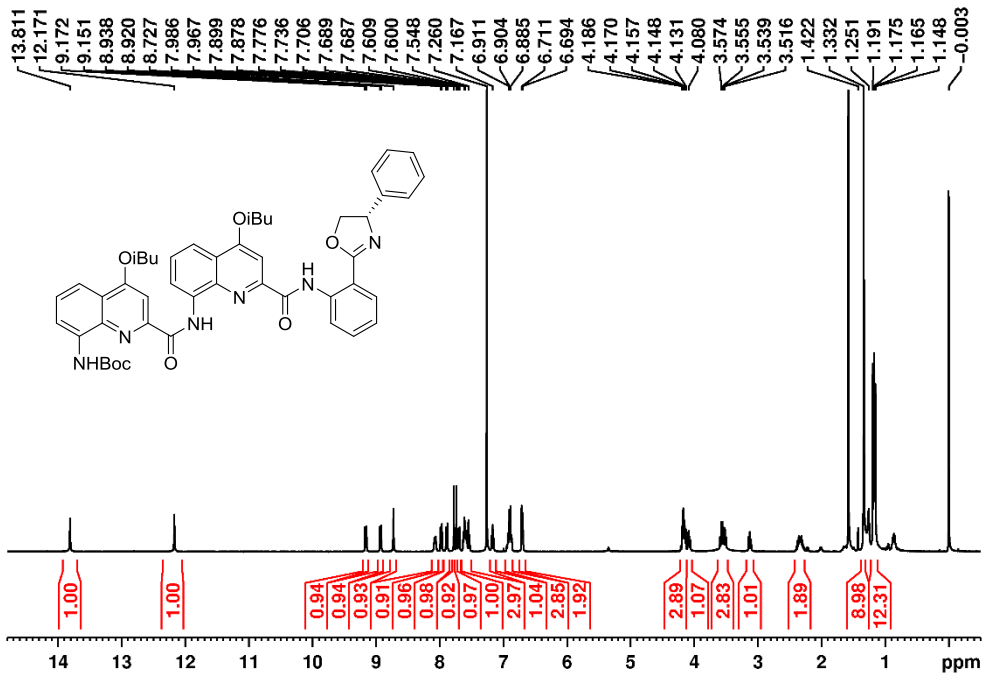

Fig. S12 ^{1}H NMR spectrum (400 MHz, 298 K) of the compound *S*-**6** in $CDCl_3$.

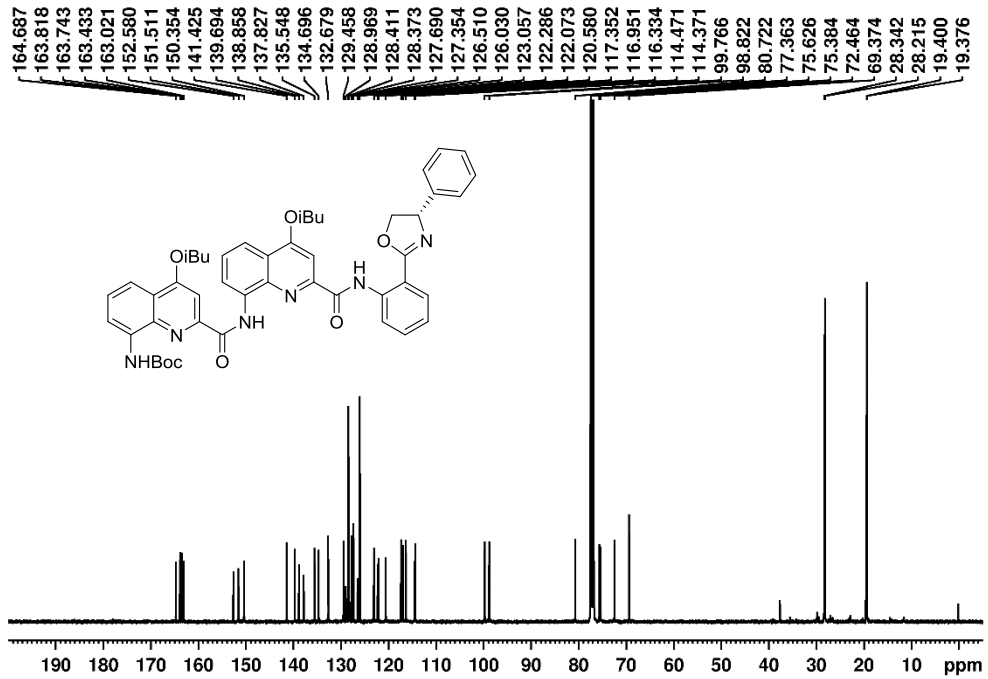

Fig. S13 ^{13}C NMR spectrum (100 MHz, 298 K) of the compound *S*-**6** in $CDCl_3$.

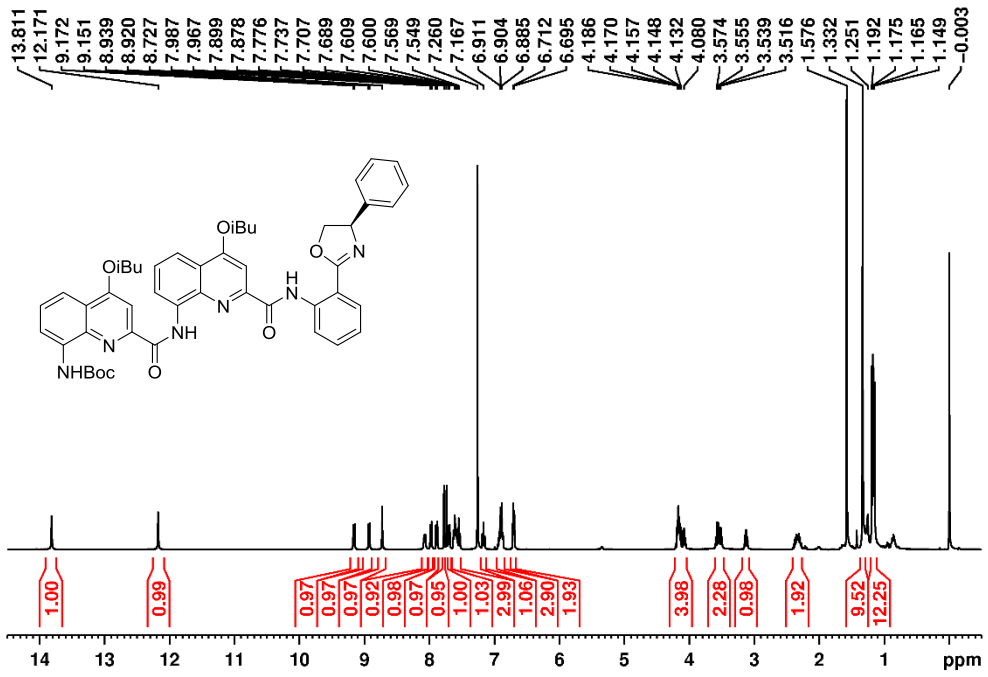

Fig. S14 ^{1}H NMR spectrum (400 MHz, 298 K) of the compound *R*-**6** in $CDCl_3$.

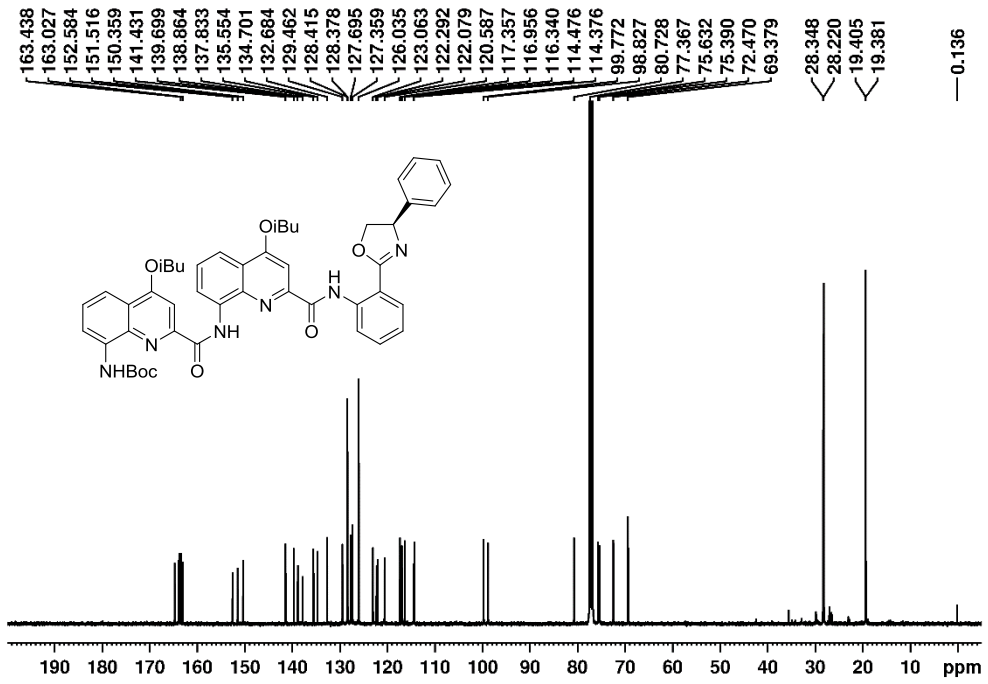

Fig. S15 ^{13}C NMR spectrum (100 MHz, 298 K) of the compound *R*-**6** in $CDCl_3$.

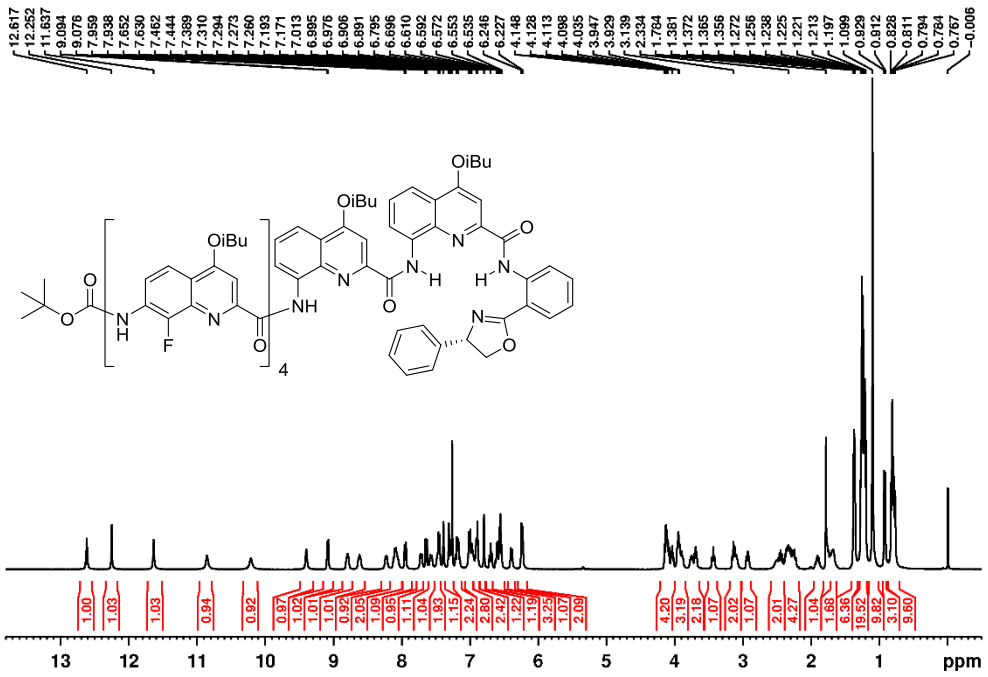

Fig. S16 ^{1}H NMR spectrum (400 MHz, 298 K) of the compound *S*-**1** in $CDCl_3$.

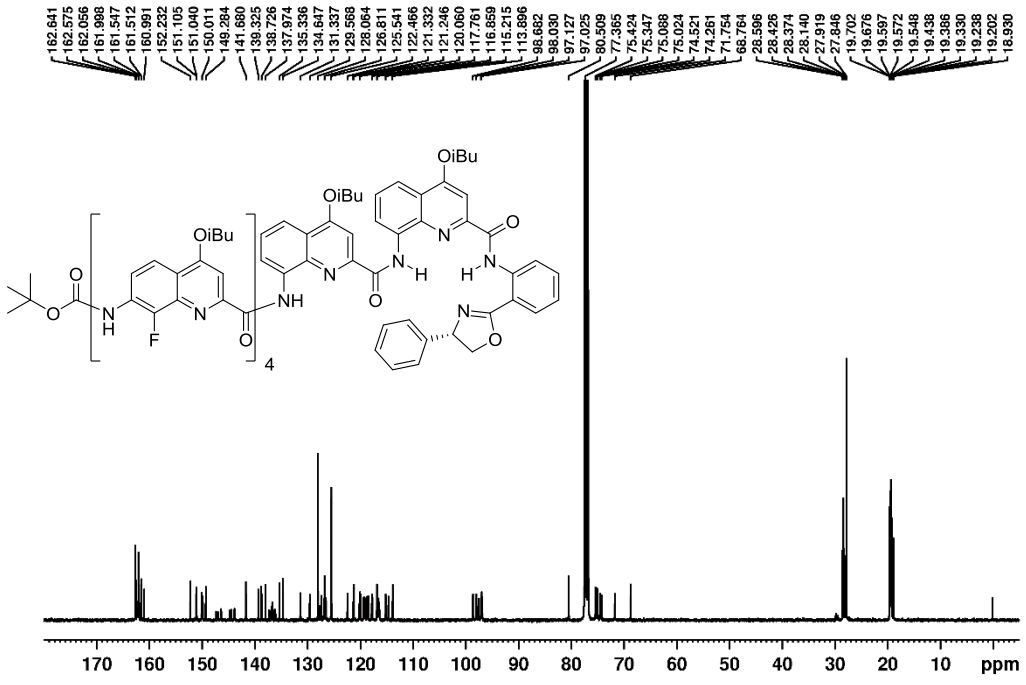

Fig. S17 ^{13}C NMR spectrum (100 MHz, 298 K) of the compound *S*-**1** in $CDCl_3$.

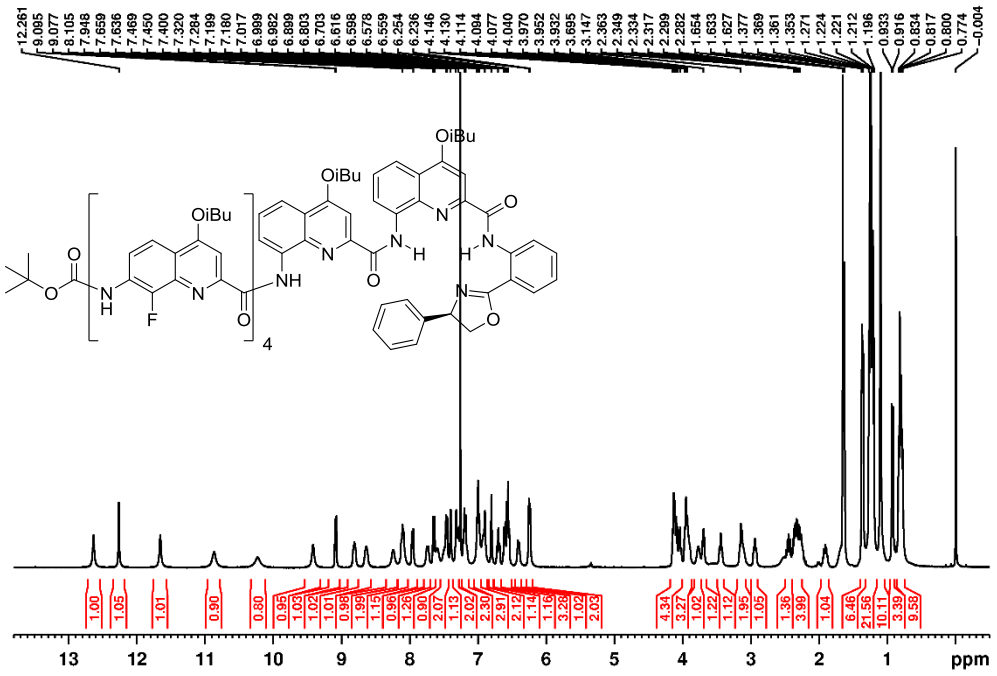

Fig. S18 ^{1}H NMR spectrum (400 MHz, 298 K) of the compound *R*-**1** in $CDCl_3$.

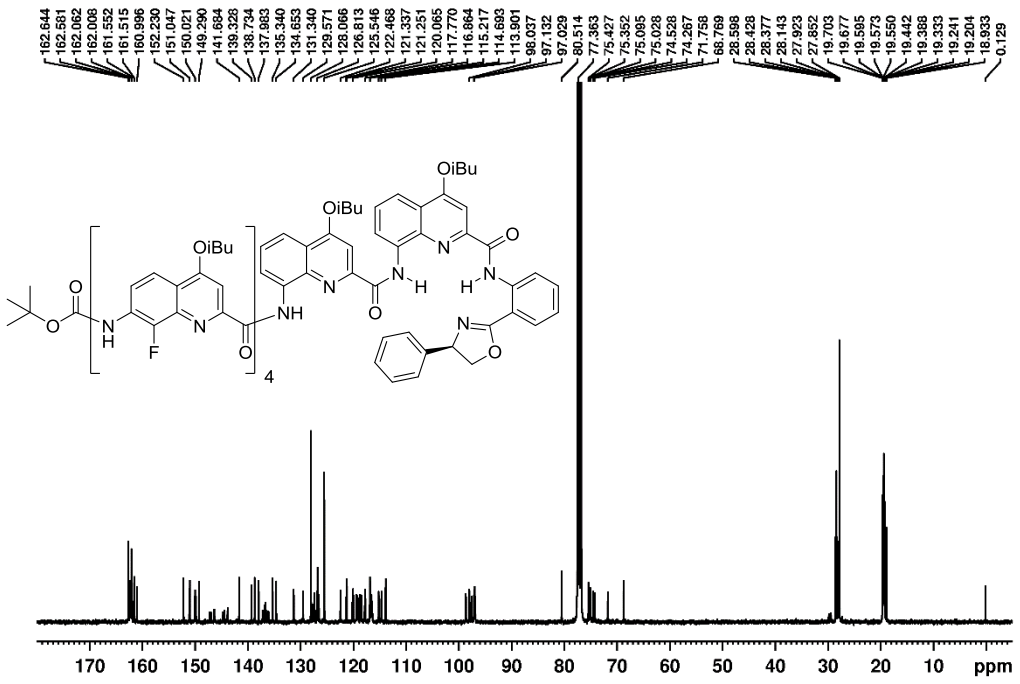

Fig. S19 ^{13}C NMR spectrum (100 MHz, 298 K) of the compound *R*-**1** in $CDCl_3$.

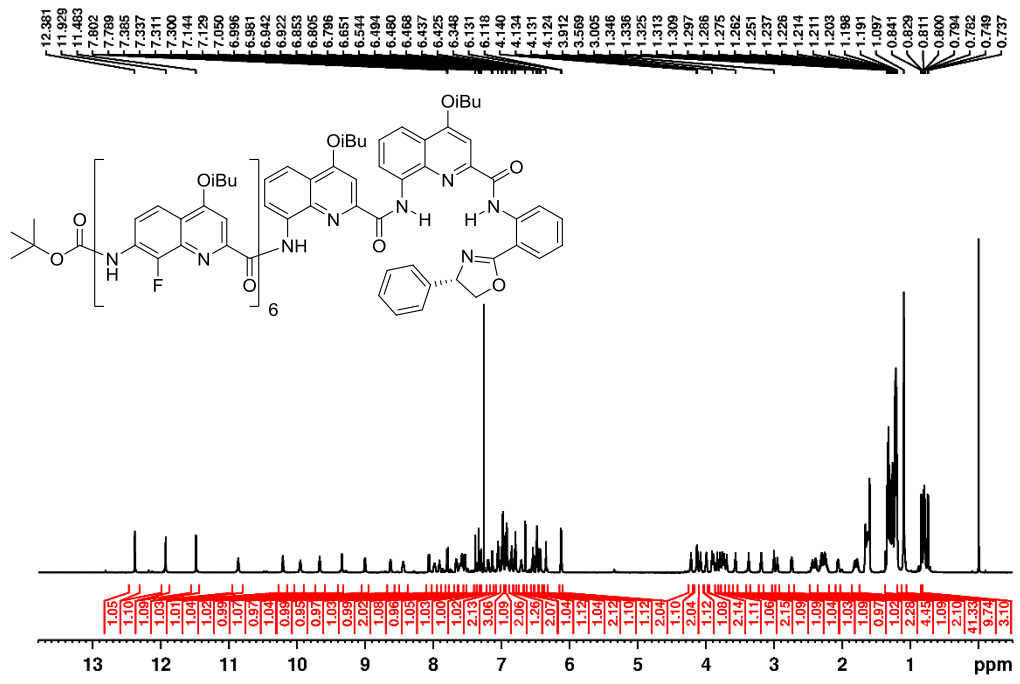

Fig. S20 ^{1}H NMR spectrum (600 MHz, 298 K) of the compound *S*-**2** in $CDCl_3$.

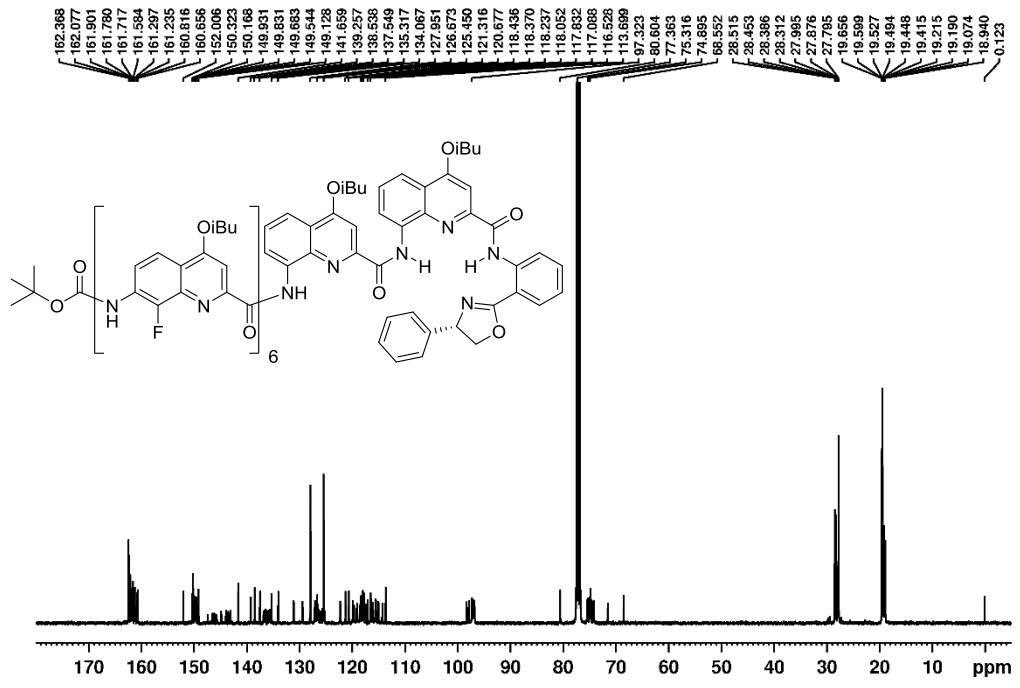

Fig. S21 ^{13}C NMR spectrum (100 MHz, 298 K) of the compound *S*-**2** in $CDCl_3$.

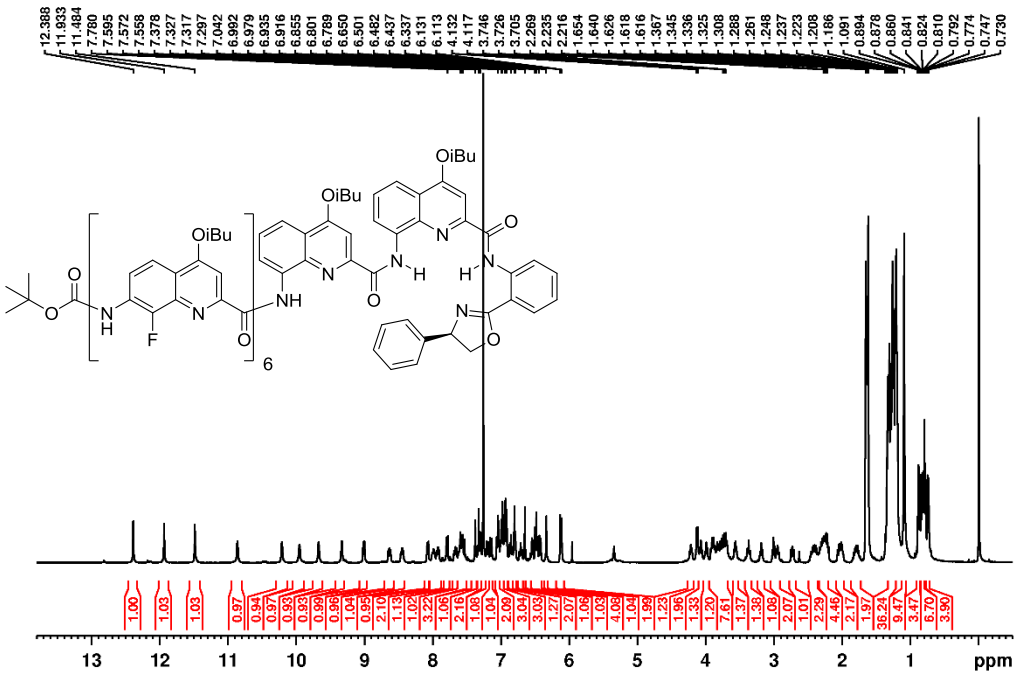

Fig. S22 ^{1}H NMR spectrum (400 MHz, 298 K) of the compound *R*-**2** in $CDCl_3$.

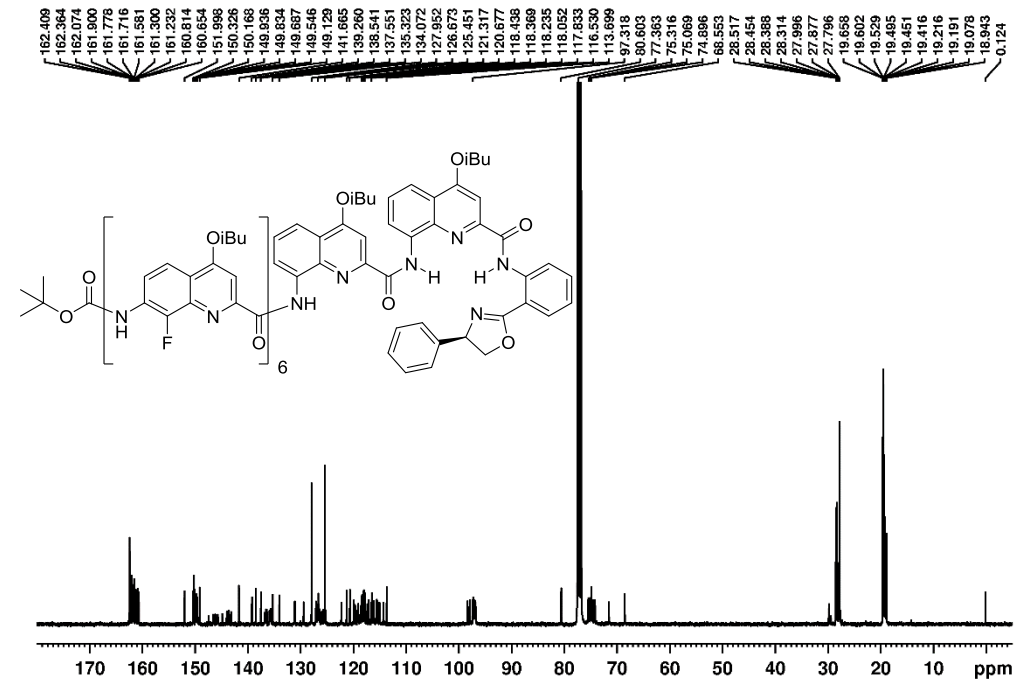

Fig. S23 ^{13}C NMR spectrum (100 MHz, 298 K) of the compound *R*-**2** in $CDCl_3$.

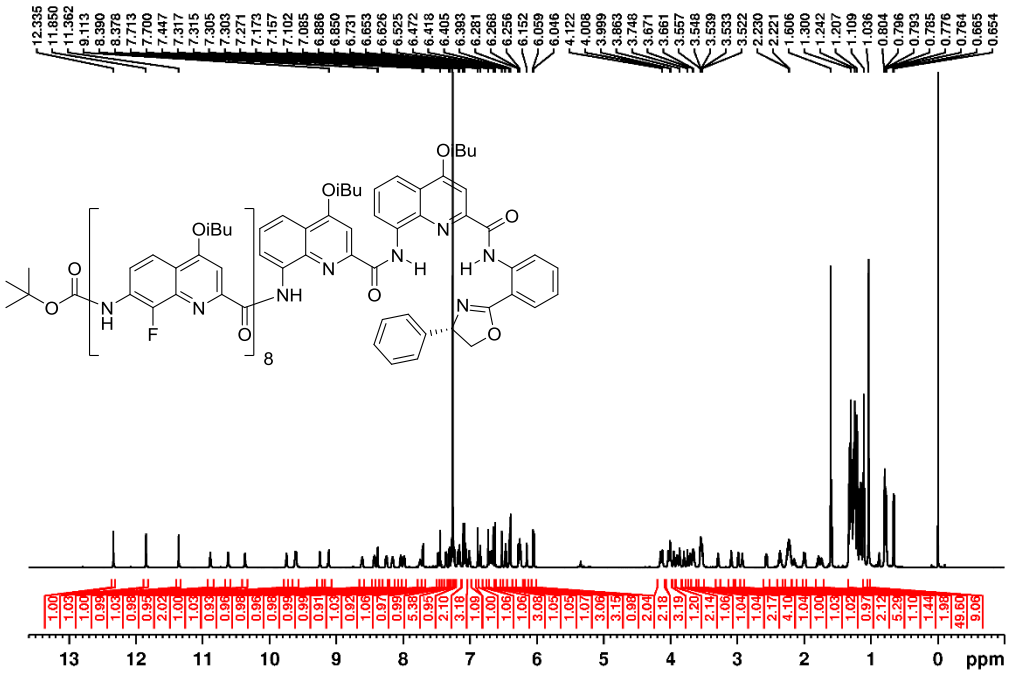

Fig. S24 ^{1}H NMR spectrum (600 MHz, 298 K) of the compound *S*-**3** in $CDCl_3$.

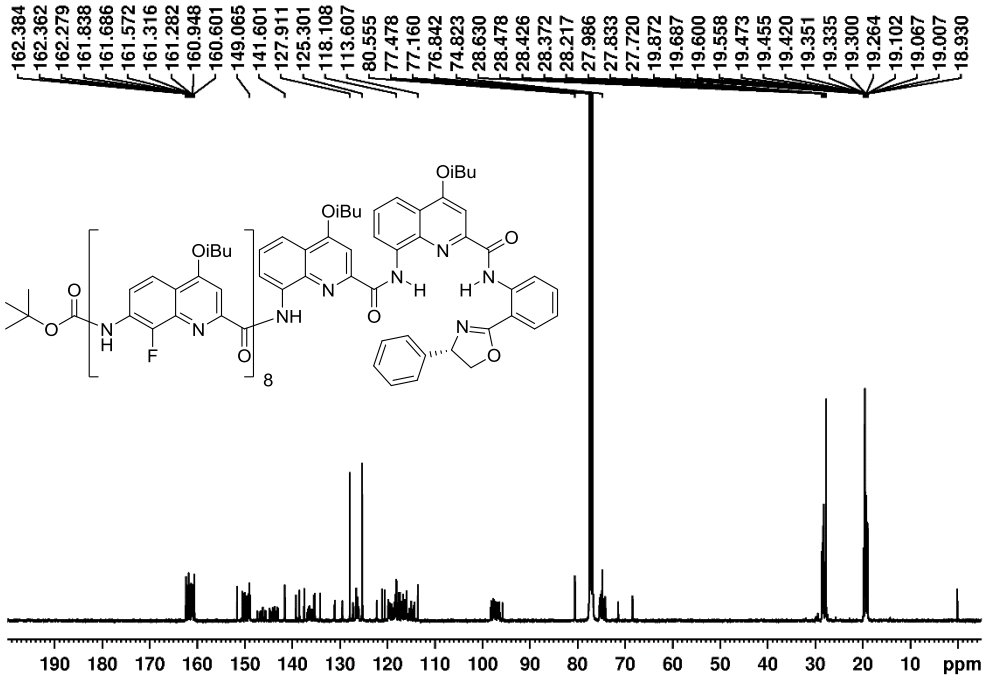

Fig. S25 ^{13}C NMR spectrum (100 MHz, 298 K) of the compound *S*-**3** in $CDCl_3$.

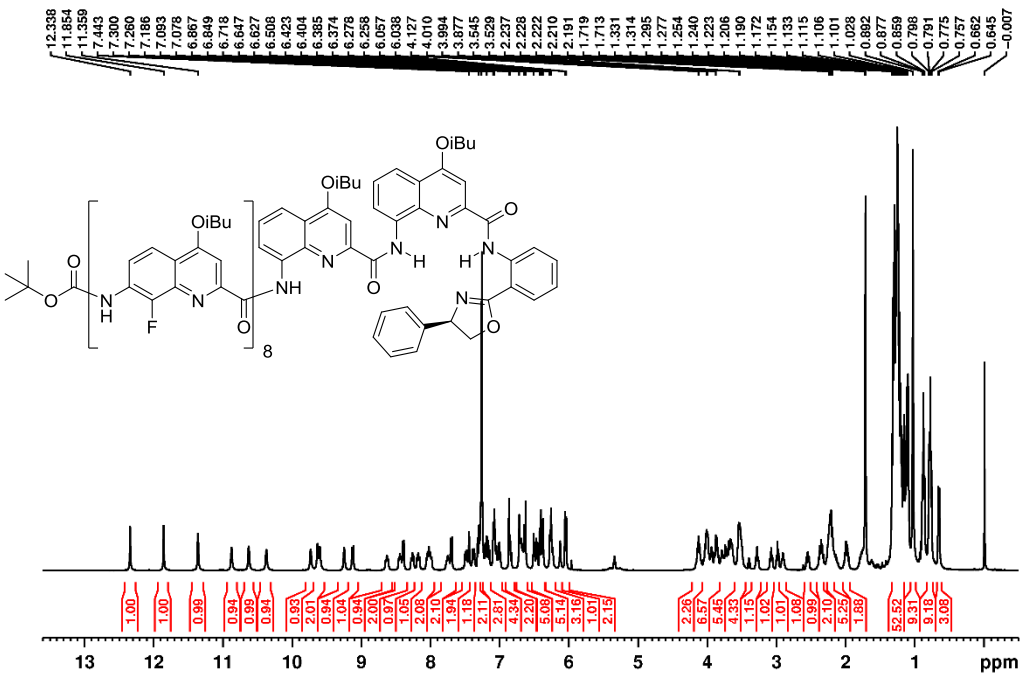

Fig. S26 ^{1}H NMR spectrum (400 MHz, 298 K) of the compound *R*-**3** in $CDCl_3$.

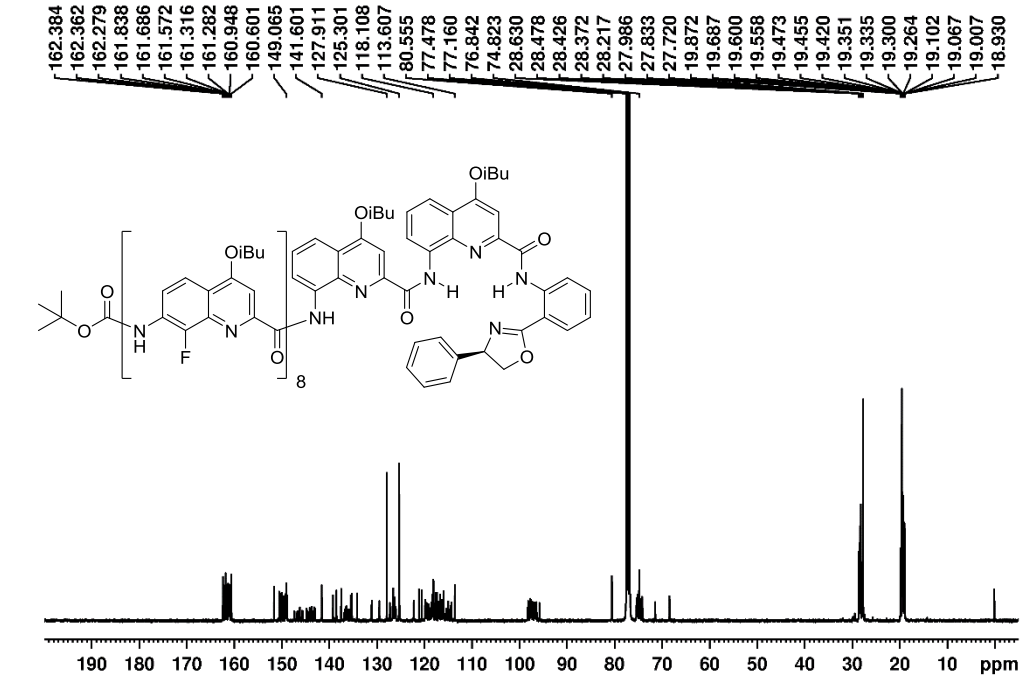

Fig. S27 ^{13}C NMR spectrum (100 MHz, 298 K) of the compound *R*-**3** in $CDCl_3$.

5. References

S1 G. M. Sheldrick, *Acta Cryst.,* 2015, **A71**,3-8.

S2 G. M. Sheldrick, *Acta Cryst.,* 2015, **C71**, 3-8.

S3 P. Müller, *Cryst. Rev.,* 2009, **15**, 57-83.

S4 A. L. Spek, *Acta Cryst.,* 2015, **C71**, 9-18.